



HAL
open science

Reappraisal of archaeal C20-C25 diether lipid (extended archaeol) origin and use as a biomarker of hypersalinity

Flore Vandier, Maxime Tourte, Cara Doumbe-Kingue, Julien Plancq, Philippe Schaeffer, Phil Oger, Vincent Grossi

► To cite this version:

Flore Vandier, Maxime Tourte, Cara Doumbe-Kingue, Julien Plancq, Philippe Schaeffer, et al.. Reappraisal of archaeal C20-C25 diether lipid (extended archaeol) origin and use as a biomarker of hypersalinity. *Organic Geochemistry*, inPress, 10.1016/j.orggeochem.2021.104276 . hal-03289759

HAL Id: hal-03289759

<https://hal.science/hal-03289759>

Submitted on 18 Jul 2021

HAL is a multi-disciplinary open access archive for the deposit and dissemination of scientific research documents, whether they are published or not. The documents may come from teaching and research institutions in France or abroad, or from public or private research centers.

L'archive ouverte pluridisciplinaire **HAL**, est destinée au dépôt et à la diffusion de documents scientifiques de niveau recherche, publiés ou non, émanant des établissements d'enseignement et de recherche français ou étrangers, des laboratoires publics ou privés.

1 **Reappraisal of archaeal C₂₀-C₂₅ diether lipid (extended archaeol)**

2 **origin and use as a biomarker of hypersalinity**

3

4 Flore Vandier^a, Maxime Tourte^b, Cara Doumbe-Kingue^b, Julien Plancq^c, Philippe

5 Schaeffer^d, Phil Oger^b, Vincent Grossi^{a*}

6

7 ^a Univ. Lyon, UCBL, ENSL, UJM, CNRS, LGL-TPE, F-69622 Villeurbanne, France

8 ^b Univ. Lyon, INSA Lyon, CNRS, UMR 5240, F-69621 Villeurbanne, France

9 ^c School of Geographical and Earth Sciences, University of Glasgow, Scotland, UK

10 ^d Univ. Strasbourg, CNRS, UMR 7177, F-67000 Strasbourg, France

11 **Author for correspondence : Vincent.grossi@univ-lyon1.fr*

12

13 **Abstract**

14 The diether core membrane lipid sesterterpanyl-phytanyl-glycerol (so-called extended
15 archaeol and often abbreviated C₂₀-C₂₅) is considered as a hallmark of Haloarchaea, a
16 clade of archaea thriving under extreme high salinities. We here report about extended
17 archaeol occurrence in different saline aquatic settings with salinity ranging from ca. 50
18 psu (5 % NaCl w/v) to saturation (ca. 350 psu). This demonstrates that this lipid is not
19 restricted to extreme saline environments but suggests a minimum salinity threshold of
20 ca. 50 psu above which C₂₀-C₂₅ is most commonly produced. The proportion of C₂₀-C₂₅
21 relative to that of archaeol (C₂₀-C₂₀) did not appear linearly dependent on the salinity of
22 the site and was potentially also influenced by pH and temperature, preventing its direct
23 use as a quantitative salinity proxy based on the present data set. An extensive literature
24 review of archaeal membrane lipid compositions further highlighted that taxonomy also

25 contributes to the distribution of this lipid in the environment and identifies Natrialbales
26 (one of the three orders of Haloarchaea) as the main source. Statistical analysis showed
27 that, among Haloarchaea, C₂₀-C₂₅ producers display pH and salinity growth optima
28 slightly higher than non-producers and are distributed within two distinct groups, one
29 composed mostly of neutrophiles and one of alkaliphiles. In contrast, the presence of
30 C₂₀-C₂₅ was not correlated to the optimal growth temperature of the strains. This
31 suggests that two confounding parameters, i.e., taxonomy and adaptation to changes in
32 salinity and/or pH, contribute to the distribution of C₂₀-C₂₅ within Haloarchaea.

33

34 **Keywords:** Halophilic archaea; extended archaeol; adaptation to pH and salinity;
35 Natrialbales

36

37 **1. Introduction**

38 Isoprenoid dialkyl glycerol diether lipids are membrane lipids unique to the Archaea.
39 Archaeol **1** (2,3-di-*O*-phytanyl-*sn*-glycerol; Fig. 1A) and its elongated homologue called
40 extended archaeol **2** (2-*O*-sesterterpanyl-3-*O*-phytanyl-*sn*-glycerol **2a** and its
41 regioisomer 2-*O*-phytanyl-3-*O*-sesterterpanyl-*sn*-glycerol **2b**; Fig. 1A) are the two main
42 types of archaeal diether lipids encountered. While **1** is globally distributed among
43 Archaea (e.g., Tourte et al., 2020), **2** was initially described only in haloalkaliphilic
44 archaea (De Rosa et al., 1982) before being detected in non-alkaline hypersaline
45 environments (Teixidor et al., 1993) and later on considered as a hallmark of halophilic
46 Euryarchaeota from the clade Haloarchaea (Dawson et al., 2012 and references therein).
47 However, few exceptions exist outside this clade (e.g., Becker et al., 2016). The extra
48 isoprenoid unit on either one of the alkyl chains in **2** compared to **1** results in an

49 asymmetric lipid that was hypothesized to induce “zip-like” archaeal membranes
50 specifically adapted to high alkalinity and strong osmotic stress (De Rosa et al., 1982).
51 The detection of **2** in sedimentary archives has been consequently associated with the
52 presence of Haloarchaea and used as a marker of hypersaline/evaporitic environments
53 (Birgel et al., 2014). Although relevant to some extent, the distribution of **2** in both
54 Archaea and environmental samples as well as its physiological and adaptive functions
55 still remain incompletely understood. For instance, this compound has been reported in
56 ancient marine sequences showing no lithological evidence of high salinities
57 (Natalicchio et al., 2017). On the other hand, preliminary results based on laboratory
58 cultures of a single Haloarchaea species (from the order Halobacteriales) have shown
59 that the relative proportion of **2** increases with increasing temperature and salinity
60 (Yamauchi, 2008), while its occurrence within a few Haloarchaea species appeared
61 related to taxonomy and optimal NaCl concentration (Dawson et al., 2012). Here, we
62 report the presence of **2** in surface sediments from aquatic environments with diverse
63 salinities, and reinvestigate its occurrence in (halo)archaea based on an extensive
64 literature survey to better constrain its biological origin and potential use as a
65 (paleo)environmental indicator.

66

67 **2. Material and Methods**

68 2.1. Sediment samples and lipid analysis

69 Surface sediments coming from 31 sites with a salinity ranging from 0 practical salinity
70 unit (psu) to saturation (ca. 350 psu) were investigated for the presence of **1** and **2**
71 (Table S1). The different sites include lakes from the Canadian Prairies (Plancq et al.,
72 2018) and the Tibetan Plateau (Wang et al., 2020), salterns from France (Camargue) and

73 Argentina (Valdes Peninsula) and saline ponds from Guadeloupe (Huguet et al., 2015).
74 Some sediments have been analyzed in previous studies while other were specifically
75 considered for the present work (Table S1). Sediment samples were freeze-dried and
76 extracted ultrasonically [methanol (MeOH) x2, dichloromethane (DCM)/MeOH (1:1,
77 v/v) x2, DCM x2] or using an automated solvent extractor (Huguet et al., 2015; Plancq
78 et al., 2018). The total lipid extracts were chromatographed over a silica gel column
79 with hexane (Hex), Hex/DCM (1:1, v/v), Hex/ethyl acetate (3:1, v/v), and DCM/MeOH
80 (1:1, v/v) as eluents. The third fraction, which contained free alcohols, was silylated
81 with pyridine/N,O-bis(trimethylsilyl)trifluoroacetamide (1:1, v/v) and analyzed by gas-
82 chromatography - mass spectrometry (GC-MS) using an Agilent 6890 gas
83 chromatograph coupled to an Agilent 5975C mass spectrometer. Compounds were
84 injected on column and separated on a HP5-MS capillary column (30 m × 0.25 mm ×
85 0.25 μm) using the following GC oven temperature program: 60 °C held for 0.5 min,
86 20 °C min⁻¹ to 130 °C then 4 °C min⁻¹ to 300 °C held for 45 min. The temperature of the
87 on-column injector was programmed as followed: 60 °C held for 0.5 min, 200 °C min⁻¹
88 to 300 °C held for 1 min. Total Ion Current (TIC) and Selected Ion Monitoring (SIM) of
89 the ions m/z 130, 131, 426 and 496 (specific of silylated derivatives of **1** and **2**; Teixidor
90 et al., 1993) were recorded. Due to the low amount of **2** and/or compounds coeluting
91 with **1** in some samples, the abundance of **2** relative to **1+2** (R) was determined from the
92 peak area measured on the SIM chromatograms, with $R = \frac{2}{1+2} \times 100$. It should be
93 noted, however, that when both measurements were possible, SIM and TIC signals
94 yielded comparable R values (Table S1).

95

96 2.2. Literature survey and statistical analyses

97 Information on the membrane lipid compositions of all Archaea species reported in the
98 literature was collected (N = 450). To estimate the influence of growth parameters on
99 the production of **2**, Haloarchaea (N = 277) were sorted between **2**-positive and **2**-
100 negative species and their optimal growth conditions (salinity, pH and temperature)
101 were compared using a non-parametric test on medians performed with the Python
102 statistical package, as data were not normally distributed. Medians were considered
103 significantly different when *P*-values were below 0.05.

104

105 **3. Results and Discussion**

106 Compounds **1** and **2** were detected in 19 and 10 out of the 31 samples analyzed,
107 respectively. Other isoprenoid diether lipids [e.g., (macro)cyclic or hydroxylated**1**] were
108 not detected besides **1** and **2**. Among the 19 lakes where **1** was observed, **2** was detected
109 in all sites with a salinity around or above 50 psu, yielding R values between 1.7 and
110 11.3 %, and was not detected in lakes with a salinity lower than 50 psu except in one
111 saline pond from Guadeloupe with a salinity of ca. 41 psu (Fig. 1B; Table S1). Although
112 sediments from hypersaline ponds with the highest salinity (ca. 350 psu, close to
113 saturation level) displayed the highest proportions of **2** (R values of ca. 11 %), similar
114 proportions of **2** were also observed in sites with a salinity between 70 and 210 psu (Fig.
115 1B). These results support **2** as a biomarker of hypersaline environments as previously
116 suggested (Teixidor et al., 1993; Birgel et al., 2014), but further show that this
117 biomarker is not restricted to extreme saline environments, extending its use to settings
118 with a salinity down to ca. 40-50 psu. This is in line with the occurrence of **2** in
119 Miocene shales, marls and carbonates which are supposed to have formed under non-
120 extreme conditions of salinity (Natalicchio et al., 2017). The proportion of **2** did not

121 appear linearly dependent on salinity (Fig. 1B), preventing the definition of a
122 quantitative salinity proxy given the present data set. It is possible, however, that some
123 uncertainties linked to the ways salinity was measured for the different sites (Table S1)
124 may have obscured such a potential linear relationship between the relative proportion
125 of **2** and salinity. On the other hand, the possibility that a sediment sample reflects
126 different salinity conditions than those at the time of sampling is not likely since only
127 the surficial sediments were analyzed and none of the ‘low-salt’ sediments in which **2**
128 was detected enclosed evaporites which could have attested from past hypersaline
129 conditions. It may also be envisaged that the occurrence of **2** further depends on other
130 environmental parameters such as pH or temperature. Because these limnological
131 parameters were not available for all the studied sites (Table S1), their potential
132 influence on the occurrence of **2** could only be partially investigated (Fig. S1). Still, for
133 the limited set of data available, a potential influence of both variables on the proportion
134 of **2** was noticed. R seemed to decrease with increasing in-situ temperature (in the range
135 15-30 °C; Fig. S1A and Table S1) which contrasts with previous observations made
136 using laboratory cultures of a single Haloarchaea species (Yamauchi, 2008). On the
137 other hand, **2** was detected in sediments with pH values ranging from 7.5 to 9.4 (Fig.
138 S1B and Table S1), pointing towards different pH conditions of production. Lastly, our
139 analyses only considered the occurrence of **1** and **2** under their free forms [i.e., as core
140 lipids (CL) without polar heads] and did not take into account the potential co-
141 occurrence of these diethers as intact polar lipids (IPL), as found in living biomass.
142 However, considering that **1** and **2** IPL are likely to exhibit similar polar heads, their
143 hydrolysis rates during diagenesis are expected to be close to each other, thus limiting
144 potential biases reflected in the R ratio based on CL analysis. Whether or not this ratio

145 can become a quantitative environmental proxy remains to be further investigated. It
146 would be of particular interest to determine if the biosynthesis of **2** scales with salinity
147 (or other environmental parameters) within individual producers, and/or if the relative
148 abundance of archaeal species producing this compound scales with salinity (or other
149 variables).

150

151 To further explore potential adaptive functions of **2** towards salinity and other growth
152 parameters, we looked for its occurrence among all the archaeal membrane lipid
153 compositions available in the literature (N= 450). It should be emphasized that all
154 literature data was not homogeneous in the sense that some studies focused on IPL,
155 whereas other studies reported CL compositions obtained after hydrolysis of total lipid
156 extracts. Since our survey considered both IPL and CL, it should not be biased by the
157 heterogeneity of the literature data. Compound **2** was reported in only 91 out of 450
158 species, with 87 species belonging to the three orders of Haloarchaea, i.e., the
159 Halobacteriales, Haloferacales and Natrilbales. The 4 additional species producing **2**,
160 namely, *Methanomassilicoccales lyminyensis*, *Methanolobus tindarius*, *Methanosarcina*
161 *barkeri* and *Methanosarcina mazei*, were randomly distributed within non-halophilic
162 methanogens (De Rosa et al., 1986; Grant and Ross, 1986; Becker et al., 2016).

163 Therefore, we focused our analysis on Haloarchaea (N= 277; Fig. 2A). Compound **2**
164 was identified in the majority of currently known Natrilbales (51 out of 78 species, 16
165 out of 22 genera), but was more sporadically reported in Halobacteriales (32 out of 90
166 species, 14 out of 31 genera) and Haloferacales (6 out of 109 species, 2 out of 18
167 genera, i.e., *Halorubrum* and *Halalkaliarchaeum*). Such distinct distributions of **2**
168 between the three Haloarchaea orders support the idea that factors controlling its

169 biosynthesis are dependent on taxonomy (Dawson et al., 2012). Its wide distribution
170 within Natrialbales would indicate that the ability to synthesize this compound is a
171 common and ancestral feature of all the species of this order, while its patchy
172 distribution within Haloferacales and Halobacteriales would suggest that members of
173 these orders have sporadically gained this biosynthetic ability by horizontal gene
174 transfers or spontaneous emergence. Another hypothesis to explain the distribution of **2**
175 within Haloarchaea is that the ability to synthesize this lipid emerged and conferred
176 increased fitness under peculiar environmental conditions, and was thus maintained.
177 In an effort to disentangle the contribution of taxonomy vs. stress response in the
178 occurrence of **2** in Haloarchaea, we gathered from the literature the in-lab optimal
179 growth conditions of all species with described membrane lipid compositions (Fig. 2B).
180 To identify putative subgroups that might for instance result from the aforementioned
181 influence of taxonomy, we represented our data using violin plots instead of typical box
182 plots. Unlike the latter, violin plots represent the probability of a data point to be in a
183 certain region of the plot (e.g., the larger the region the more data points it contains) and
184 thus better depicts the data set distribution. Results showed that Haloarchaea
185 synthesizing **2** grow optimally at significantly higher pH (7.45 vs. 7.30, P -value =
186 0.015) and salinity (200 vs. 190 psu, P -value = 0.035) than non-producing species (Fig.
187 2B). However, although significant, these differences appeared rather small to support a
188 major influence of growth pH and/or salinity on the biosynthesis of **2**. This nonetheless
189 hints that **2** may have played a role in the (long-term) adaptation of Haloarchaea to pH
190 and salinity variations. Looking more closely at their optimal growth conditions, species
191 capable of the synthesis of **2** are distributed within two distinct groups: one composed
192 mostly of neutrophilic Haloarchaea (median pH = 7.2) and one of alkaliphilic

193 Haloarchaea, mostly Natrialbales (median pH = 9.2; Figure 2B). Such a bimodality
194 suggests that two confounding parameters, i.e., taxonomy and adaptation, might
195 contribute to the distribution of **2** within Haloarchaea. For instance, **2** might support
196 adaptation towards extreme pH in Natrialbales, while it might provide other yet
197 unknown advantage in Haloferacales and Halobacteriales.

198 Our statistical analysis further showed that the occurrence of **2** is not correlated to the
199 optimal growth temperature of Haloarchaea (P -value = 0.523; Fig. 2B). This suggests
200 that temperature have not exerted a significant control on the biosynthesis of **2** during
201 the long-term evolution of this clade (Fig. S1A). It may not preclude, however, that
202 temperature may influence the proportion of this lipid in the membrane of the archaeal
203 producers during short-term acclimatisation (Yamauchi, 2008; Fig. S1A).

204

205 The current set of archaeal lipid compositions further places Haloarchaea as the main
206 producers of **2**. As the vast majority of currently known Haloarchaea are unable to
207 thrive at salinity below 100 psu, the presence of **2** in sediments with salinity from ca. 40
208 to 100 psu is intriguing (Fig. 1B). However, **2** has been reported in non-halophilic
209 species distinct from Haloarchaea (i.e., in non-halophilic methanogens; De Rosa et al.,
210 1986; Grant and Ross, 1986; Becker et al., 2016) and the lipid composition of numerous
211 archaeal species is yet uncharacterized. The possibility that a whole range of producers
212 of **2** besides Haloarchaea may contribute to the pool of this lipid biomarker in
213 environments with contrasted salinity thus cannot be ruled out. On the other hand,
214 Haloarchaea have been observed in low or non-extreme saline environments such as
215 estuaries (Purdy et al., 2004; Singh et al., 2010), sulfur-rich springs (Elshahed et al.,
216 2004) or thiotrophic microbial mats (Jessen et al., 2016), suggesting that some (yet

217 undescribed) low salt-tolerant Haloarchaea might be responsible for the production of 2
218 in settings with moderate salinity.

219 In spite of the still fragmented information currently available on the biosynthesis
220 (producers and conditions) of extended archaeol, the present study encourages further
221 investigation of the physiological role, environmental occurrence and potential use as
222 (paleo)environmental indicator of this puzzling lipid.

223

224 **Acknowledgments**

225 We thank Dr. Mingda Wang for his valuable help in gathering the environmental
226 parameters of the Tibetan lakes and Dr Philippe Cuny for providing the sediments from
227 salterns. We thank two anonymous reviewers for their comments which greatly
228 improved the manuscript. We are grateful to the CNRS Interdisciplinary program MITI
229 ‘Adaptation du vivant à l’environnement’ (project Adaphalo 2020-2021) and the ENS
230 Lyon for their financial support.

231

232 **References**

- Becker, K.W., Elling, F.J., Yoshinaga, M.Y., Söllinger, A., Urich, T., Hinrichs, K.-U.,
2016. Unusual butane- and pentanetriol-based tetraether lipids in
Methanomassiliicoccus luminyensis, a representative of the seventh order of
Methanogens. Applied and Environmental Microbiology 82, 4505-4516.
- Birgel, D., Guido, A., Liu, X., Hinrichs, K.-U., Gier, S., Peckmann, J., 2014.
Hypersaline conditions during deposition of the Calcare di Base revealed from
archaeal di- and tetraether inventories. Organic Geochemistry 77, 11-21.

- Cui, H.-L., Dyall-Smith, M.L., 2021. Cultivation of halophilic archaea (class *Halobacteria*) from thalassohaline and athalassohaline environments. *Marine Life Science & Technology* 3, 243-251.
- Dawson, K.S., Freeman, K.H., Macalady, J.L., 2012. Molecular characterization of core lipids from halophilic archaea grown under different salinity conditions. *Organic Geochemistry* 48, 1-8.
- De Rosa, M., Gambacorta, A., Gliozzi, A., 1986. Structure, biosynthesis, and physicochemical properties of archaeobacterial lipids. *Microbiological Reviews* 50, 70-80.
- De Rosa, M., Gambacorta, A., Nicolaus, B., Ross, H.N.M., Grant, W.D., Bu'Lock, J.D., 1982. An asymmetric archaeobacterial diether lipid from alkaliphilic halophiles. *Microbiology* 128, 343-348.
- Elshahed, M.S., Najar, F.Z., Roe, B.A., Oren, A., Dewers, T.A., Krumholz, L.R., 2004. Survey of archaeal diversity reveals an abundance of Halophilic archaea in a low-salt, sulfide- and sulfur-rich spring. *Applied and Environmental Microbiology* 70, 2230-2239.
- Ernst, R., Ejsing, C.S., Antonny, B., 2016. Homeoviscous adaptation and the regulation of membrane lipids. *Journal of Molecular Biology, Molecular Biology of Membrane Lipids* 428, 4776-4791.
- Grant, W.D., Ross, H.N.M., 1986. The ecology and taxonomy of halobacteria. *FEMS Microbiology Reviews* 2, 9-15.
- Hou, J., Tian, Q., Wang, M., 2018. Variable apparent hydrogen isotopic fractionation between sedimentary *n*-alkanes and precipitation on the Tibetan Plateau. *Organic Geochemistry* 122, 78-86.

- Huguet, A., Grossi, V., Belmahdi, I., Fosse, C., Derenne, S., 2015. Archaeal and bacterial tetraether lipids in tropical ponds with contrasting salinity (Guadeloupe, French West Indies): Implications for tetraether-based environmental proxies. *Organic Geochemistry* 83-84, 158-169.
- Jessen, G.L., Lichtschlag, A., Struck, U., Boetius, A., 2016. Distribution and composition of thiotrophic mats in the hypoxic zone of the Black Sea (150-170 m water depth, Crimea Margin). *Frontiers in Microbiology* 7, 1011.
- Li, C., Zhang, Q., Kang, S., Liu, Y., Huang, J., Liu, X., Guo, J., Wang, K., Cong, Z., 2015. Distribution and enrichment of mercury in Tibetan lake waters and their relations with the natural environment. *Environmental Science and Pollution Research* 22, 12490-12500.
- Natalicchio, M., Birgel, D., Peckmann, J., Lozar, F., Carnevale, G., Liu, X., Hinrichs, K.-U., Dela Pierre, F., 2017. An archaeal biomarker record of paleoenvironmental change across the onset of the Messinian salinity crisis in the absence of evaporites (Piedmont Basin, Italy). *Organic Geochemistry* 113, 242-253.
- Plancq, J., Cavazzin, B., Juggins, S., Haig, H.A., Leavitt, P.R., Toney, J.L., 2018. Assessing environmental controls on the distribution of long-chain alkenones in the Canadian Prairies. *Organic Geochemistry* 117, 43-55.
- Purdy, K.J., Cresswell-Maynard, T.D., Nedwell, D.B., McGenity, T.J., Grant, W.D., Timmis, K.N., Embley, T.M., 2004. Isolation of haloarchaea that grow at low salinities. *Environmental Microbiology* 6, 591-595.
- Singh, S.K., Verma, P., Ramaiah, N., Chandrashekar, A.A., Shouche, Y.S., 2010. Phylogenetic diversity of archaeal 16S rRNA and ammonia monooxygenase genes

from tropical estuarine sediments on the central west coast of India. *Research in Microbiology* 161, 177-186.

Teixidor, P., Grimalt, J.O., Pueyo, J.J., Rodriguez-Valera, F., 1993. Isopranyl glycerol diethers in non-alkaline evaporitic environments. *Geochimica et Cosmochimica Acta* 57, 4479-4489.

Tourte, M., Schaeffer, P., Grossi, V., Oger, P.M., 2020. Functionalized membrane domains: An ancestral feature of Archaea? *Frontiers in Microbiology* 11, 526.

Wang, S., Dou, H. (1998). *A Directory of Lakes in China*. Beijing: Science Press.

Wang, M., Liang, J., Hou, J., Hu, L., 2015. Distribution of GDGTs in lake surface sediments on the Tibetan Plateau and its influencing factors. *Science China Earth Science* 59, 961-974.

Wang, M., Tian, Q., Li, X., Liang, J., He, Y., Hou, J., 2020. TEX₈₆ as a potential proxy of lake water pH in the Tibetan Plateau. *Palaeogeography, Palaeoclimatology, Palaeoecology* 538, 109381.

Yamauchi, N., 2008. ESI-MS and GC-MS analyses of C₂₅-C₂₀ isoprenoidal diether originated from halophilic archaea with reference to an indicator for hypersaline environment. *Researches in Organic Geochemistry* 23-24, 123-130.

Figure legends

Figure 1. **A)** Structures of archaeol **1** and the two possible regioisomers of extended archaeol **2**; **B)** Proportion of **2** relative to **1** in superficial sediments of lakes and ponds with different salinities. The dashed line indicates a possible threshold for the presence of **2** around 40-50 psu. $R = \frac{2}{1+2} \times 100$.

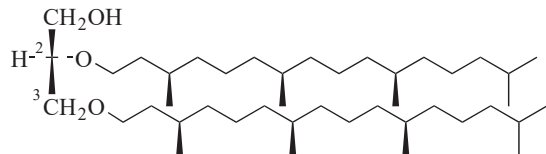
Figure 2. **A)** Archaeal phylogenetic tree (redrawn from Cui and Dyall-Smith, 2021) and average optimal growth parameters (salinity, pH and temperature) of Haloarchaea. Genera highlighted in red illustrate the presence of **2** in at least one species; genera in bold red are those for which all species were reported to produce **2**. **B)** Distribution of optimal growth parameters among Haloarchaea producing (red) or not (white) extended archaeol **2** (literature data). Violin plots include the medians (white dots), 1st and 3rd quartiles (black box limits), ranges (black whiskers) and probability densities (shape width).

Figure S1. Proportion of **2** relative to **1** in superficial sediments of lakes and ponds as a function of **A)** temperature (°C) and **B)** pH. $R = \frac{2}{1+2} \times 100$. Only samples where **1** and/or **2** were detected are represented (see Table S1). pH values in saline ponds from Guadeloupe were rough estimates based on pH paper and were thus not considered.

Table S1. Characteristics of the surface sediment samples investigated.

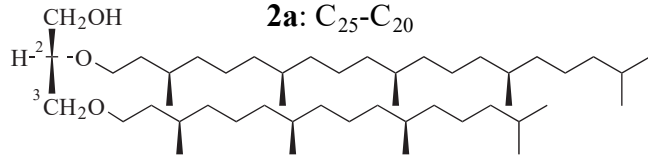
Figure 1 revised

1: Archaeol (C₂₀-C₂₀)

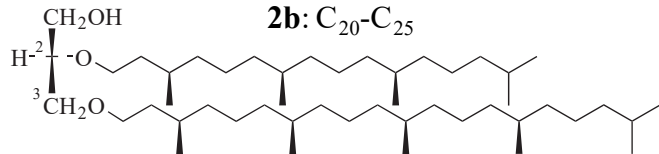


2: Extended archaeol

2a: C₂₅-C₂₀



2b: C₂₀-C₂₅



Click here to access/download;Figure;Vandier et al Fig 1 revised.pdf

